HELICON DISCHARGE EXCITED BY A PLANAR ANTENNA IN BOUNDED VOLUME

V.F. Virko, V.M. Slobodyan, K.P. Shamrai, Yu.V. Virko

Institute for Nuclear Research NAS of Ukraine, Kyiv, Ukraine

E-mails: slava.slobodyan@gmail.com, virko@mail.ru

By direct spatial measurements of wave RF magnetic fields it is confirmed that the density jumps in the helicon discharge with a flat (planar) antenna result from changes in axial modes of standing helicon waves in a limited volume. In independently produced plasma the planar antenna resistance was measured at various plasma densities n and magnetic fields B_0. In the studied range of parameters ($n/B_0 \leq 2.5\times10^{20}$ $T^{-1}m^{-3}$) the planar antenna impedance increases with the ratio n/B_0, in contrast to other types of helicon antennas. The resonances of RF power absorption, caused by standing waves excitation, for the planar antenna are observed at about two times higher values of n/B_0 than for the frame $m = 1$ antenna.

PASC: 52.50.Dg

INTRODUCTION

The helicon discharge is an effective electrodeless source of low-temperature plasma for various applications [1]. A characteristic feature of this type discharge is the abrupt changes in plasma density at monotonous changing of external parameters, such as radio frequency (RF) power, magnetic field and gas pressure [2, 3]. In the helicon mode the density jumps are due to wave nature of the discharge: those parameters are realized in which the lengths of excited helicon waves satisfy certain resonant boundary conditions. These conditions may be imposed by the discharge volume geometry, for standing waves formation, as well as by the inductive antenna design and dimensions. For instance, for the antennas exciting the first azimuthal mode $m = 1$ of helicon waves (m-azimuthal wave number), the main resonance occurs when the antenna length L_A holds a half of wavelength $\lambda/2$ [1].

As known the helicon wavelength λ decreases with increasing the ratio of plasma density to magnetic field n/B_0. Therefore, at a fixed magnetic field B_0 an abrupt increase in density at increasing RF power reduces λ and corresponds to transition to a higher mode of the standing helicon waves. On the contrary, the same density increase with increasing the magnetic field [2] compensates the field action and retains the resonant wavelength. In this case, the density rise occurs without changing the standing wave mode, but such a rise is possible only if the sufficient RF power is available. If the power is not enough to maintain the higher density, the discharge moves to a lower mode or ceases.

For excitation of azimuthally-symmetric helicon waves $m = 0$ typically one- or two-turn loop antennas, placed externally on a dielectric discharge chamber, are used. Their dimension along the magnetic field may be neglected. For this reason, these antennas have the continuous wave number spectrum and do not expose the above mentioned "antenna" resonances. Only the volume resonances or “cavity modes” remain at which the chamber length contains an integer number of $\lambda/2$. In this case, for efficient coupling to plasma the loop antenna have to be placed within the maximum of standing wave field.

Recently, to create short and wide-aperture plasma sources the inductive antennas shaped as a flat spiral placed on a plain dielectric vacuum window at the end of the discharge chamber are used [4 - 7]. It was found that at presence of magnetic field such a "planar" antenna also excited the azimuthally-symmetric helicon waves $m = 0$. But some characteristics of this discharge differ from the discharges with traditional antennas of modes $m = 1$ and $m = 0$. At a fixed RF power the gradual increasing of magnetic field in the discharge with a planar antenna is accompanied by several characteristic saw-like falls of density and finally, at some critical field, ends with breakdown the discharge into a low intensity state [8]. In this paper direct measurements of spatial distributions of the wave RF magnetic fields confirm that such density dependence in discharges with the planar antenna also is a result of changes in axial modes of standing helicon waves in a limited volume.

Besides, in modelling experiments with independently produced plasma the resistance of the planar antenna caused by a plasma load was measured at various plasma densities n and magnetic fields B_0. A comparison of the planar antenna characteristics with other types of inductive antennas used to excite the helicon discharges has been performed.

1. DISCHARGE CHARACTERISTICS AND WAVE FILD DISTRIBUTIONS

1.1. EXPERIMENTAL SETUP

Experiments were carried out in the device shown in Fig. 1. The discharge volume consisted of a metal (stainless) section (1) of 14 cm inner diameter and 14 cm in length, and a quartz chamber (2) of the same diameter and 23 cm long. The chamber was placed in a system of coils (7), which formed approximately homogeneous magnetic field up to 10 mT.

On the left end (Z = 38 cm) the chamber was closed with a metal flange-reflector (9), which had a diametric slit to let pass the two-coordinate movable probe (8) and for pumping the volume. The opposite end (Z = 0) terminated with a flat quartz window (3) of 15 mm thick. Close to the window the four-turn planar antenna (4) was placed in the form of a plain spiral with outside diameter of 12 cm and internal of 6 cm. The antenna was made of copper tube 4 mm in diameter and was water cooled. Through a standard matching device (5) the antenna was fed with RF current from the generator (6) of frequency 13.56 MHz and power up to 1 kW. The antenna current magnitude was controlled by a thermal

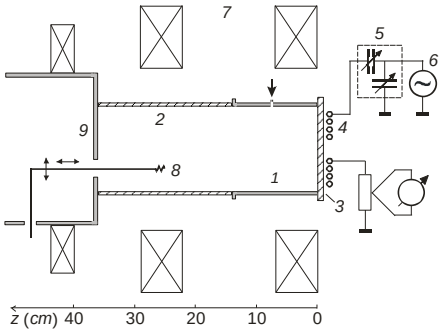

Fig. 1. Experimental setup for study the discharge with planar antenna: 1 – metal section; 2 – quartz chamber; 3 – quartz window; 4 –planar antenna; 5 – matching network; 6 – RF generator; 7 – magnetic field coils; 8 – two-coordinate probe; 9 – flange-reflector. f = 13.56 MHz, $W \le 1$ kW, p_{Ar} = 0.65 Pa, $B_0 \le 10$ mT

ammeter. Incident and reflected powers were measured by directional couplers in the RF generator.

The magnetic probe (8) was an 8-turn coil of diameter 1 cm from bare stainless steel wire 0.5 mm in diameter. The probe wires passed through a ceramic two-hole rod, which was shielded against RF fields with neuzilber tube 4 mm in diameter. The probe could move along Z axis within a distance of 32 cm and independently along the chamber diameter. Magnetic probe terminals were connected to the balance transformer which eliminated the in-phase part of signal, arising from plasma potential fluctuations, and selected out its magnetic component. After a resonance (13.56 MHz) detector the signal came to the Y-input of the recorder, which X-coordinate voltage was proportional either to the probe displacement or to the magnetic coils current, i.e. the magnetic field strength. By giving a negative bias to the probe we could also measure the ion saturation current, qualitatively proportional to plasma density.

The device was pumped out to residual pressure of 13 mPa. The working gas–argon–was let in the metal section. The pressure was measured above the vacuum pump, behind the reflecting end flange.

1.2. RESULTS AND DISCUSSION

The dependence of plasma density on external magnetic field was studied using the probe (8), which in this case was used as an ordinary Lengmuir probe. The probe was placed on the chamber axis at a position Z = 24 cm and was negatively biased to $U_p = -60$ V. Since the probe had a complex configuration and its collecting surface was not defined, it was not used for absolute measurements. Only ion saturation current to the probe was registered, that characterized the relative changes in plasma density when the magnetic field was varying. A typical appearance of this dependence at argon pressure of 0.65 Pa is shown in Fig. 2 by the solid curve. Without magnetic field a low intensity inductive discharge is observed near the antenna. In this case, the plasma does not reach the probe and probe current is absent. With increasing the field the discharge becomes

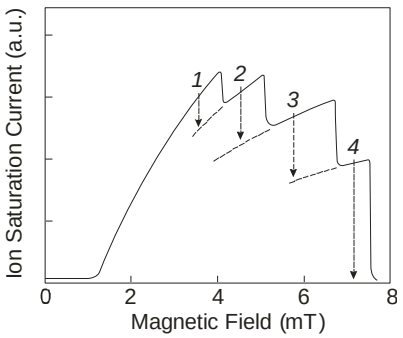

Fig. 2. Ion current dependence on magnetic field. The probe is placed on the axis at Z = 24 cm, U_P = -60 V, absorbed power W = 650 W at B_0 = 5 mT, argon pressure p_{Ar} = 0.65 Pa

more intense and extends along the axis. Because increasing the volume ionization the probe current rises. Further increase of the magnetic field is accompanied by several stepped drops of plasma density and, in excess of the critical field value (in this case B_{cr} = 7.5 mT) the discharge breaks up.

Note, that in these experiments the RF energy absorption in plasma changes simultaneously and, because breach of matching the generator anode current and its output power also vary. For this reason, the matching and generator regime were preliminarily set so that at B_0 = 5 mT the absorbed power was W = 650 W. Then, the matching and the output power changed spontaneously, namely: with increasing B_0 the reflection decreased and the output power increased. After the final discharge breakdown the reflected power strongly increased and the discharge could be recovered only by reducing the magnetic field.

Using the magnetic probe the axial distributions of the wave RF magnetic field, B_Z, corresponding to separate steps of the curve see in Fig. 2 were studied. At the same fixed conditions regarding the generator output, matching and gas pressure as see in Fig. 2, the magnetic field was increased from zero to one of the values shown see in Fig. 2 by dashed arrows (B_0 = 3.5, 4.5, 5.8 and 7.2 mT). Then, at each of these values B_0 the probe was moving from the extreme position Z = 33 cm towards the antenna (Z = 0). Initial distributions of the probe signal, which is proportional to the RF magnetic field amplitude, for each value B_0 are shown in Fig. 3 by the dashed curves. Since the

probe has a significant size (1 cm in diameter), at some its positions (Z = 25, 17, 11.5 and 13 cm) due to a caused by the probe disturbance a jump of the discharge regime happens and the probe signal sharply changes, as is shown by the arrows. After the jump the following signal dependences on coordinate, shown in Fig. 3 by the solid curves, remain the same as the probe moves in both directions between Z = 1.5 cm and Z = 33 cm. In the latter case, at B_0 = 7.2 mT and the probe position Z = 13 cm the discharge finally breaks down and, with approaching to Z = 0 only a vacuum field of the inductive antenna is observed. Note, that in Fig. 3 the amplitude distributions in an inaccessible area between the extreme position of the probe (Z = 33 cm) and the reflecting flange (Z = 38 cm) were drawn with pointed curves by extrapolation.

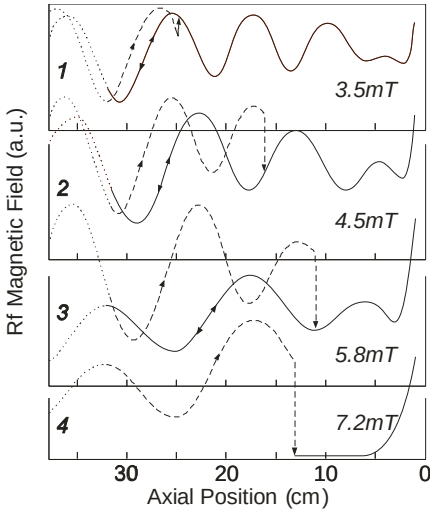

Fig. 3. Axial distributions of standing helicon waves amplitude at different magnetic fields. Curves 1 – 4 correspond to points 1 – 4 in see Fig. 2

Note some features of the spatial amplitude distributions of the RF magnetic field in see Fig. 3. Firstly, a finite value of the standing wave coefficient and its decrease with distance from the flange-reflector indicates that the mixed helicon waves propagate and the spatial absorption of their energy in plasma takes place. Secondly, the difference from zero of alternative B_Z field on the surface of reflecting flange (9) is likely due to its finite resistance (stainless steel tin) and to the presence of diametric slot for the probe pass, so that the flange conductivity is complex. Finally, on the opposite side of the chamber, near Z = 0, if we reject the own vacuum field of inductive antenna, we can see that the amplitude of the standing wave field extrapolates to zero on the dielectric window surface, that is rather unexpected to the wave excitation region.

It is important to emphasize that with each new, larger value of the external magnetic field, B_0, the unperturbed (before the jump) distribution of amplitude $B_Z(Z)$ corresponds to the basic standing wave mode, observed at the previous value of magnetic field after the mode jump. That is, the dashed curve accurately reproduces the solid curve of the previous graph. Thus, as it follows from see Figs. 3, 2 in an axially limited volume the discharge can exist only in discrete regimes, each corresponding to a particular longitudinal standing helicon wave mode and which parameters are linked by the dispersion law. Curves 1...4 see in Fig. 3 correspond to transitions from 6th to 3rd axial modes, after which the discharge breakdown takes place. Obviously, that in a shorter system with less distance between the antenna and the reflecting surface, the number of jumps would be smaller, since the shortest possible wavelength corresponds to a lower mode number.

Apparently, the regime jumps and discharge breakdown are caused by limited power of RF generator that

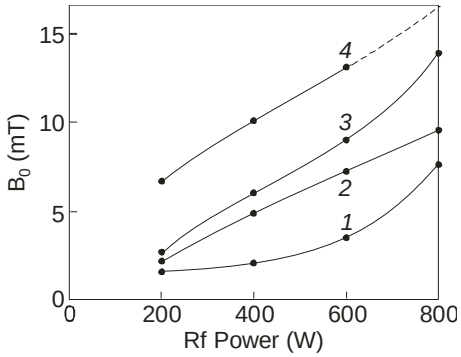

Fig. 4. Dependence of critical magnetic field corresponding to the discharge breakdown on RF power at different argon pressures. Curves 1 – 4 correspond to argon pressures of 0.65, 1.3, 3.3 and 10 Pa

does not provide the sufficient density to maintain the short wavelength (higher mode) at a larger magnetic field. Indeed, it was found [6] that increasing RF power significantly increased the critical magnetic fields corresponding to the density jumps and discharge breakdown. Fig. 4 shows the dependence of critical

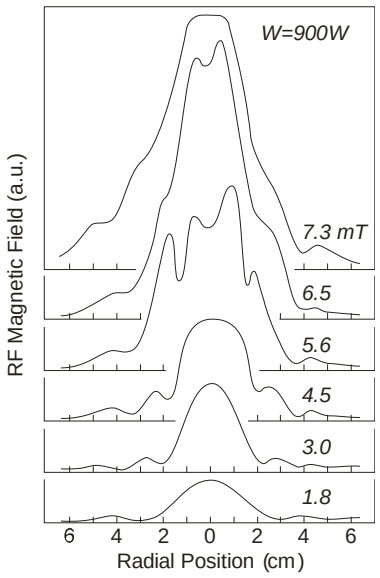

Fig. 5. Radial distribution of RF magnetic field B_Z at different external magnetic fields B_0 (p_{Ar} = 0.65 Pa, W = 900 W)

magnetic fields of the discharge breakdown on the generator output at various argon pressures. Curves 1…4 correspond to pressures 0.65, 1.3, 3.3 and 10 Pa. For the last curve at the power 800 W the critical field value exceeded the maximum field available in the experiment that is shown by the dashed line see in Fig. 4.

Comparison of the experimentally measured standing waves lengths with the theoretical helicon dispersion of the azymuthal mode $m = 0$ is complicated by presence in the discharge of higher radial modes. Fig. 5 shows the radial profiles of the RF magnetic field amplitude, $B_Z(r)$, in the chamber cross-section $Z = 24$ cm at argon pressure of 0.65 Pa and absorbed power 900 W at various external magnetic fields B_0. Since the probe position on Z-axis was fixed, some of the profiles see in Fig. 5 were obtained out of standing wave maximum. Nevertheless, see from Fig. 5 the presence of the higher radial modes for all represented values of B_0 is evident. The excitation of higher order radial modes in the helicon discharge with a planar antenna was also observed in [7]. There it was considered to be related to the magnetic field configuration and the radial density profile. See in Fig. 5 a significant concentration of RF fields in the near-axis area is seen, but the plasma density distribution in our case was much wider: on the antenna diameter (12 cm) the ion saturation current decreased by about two times.

2. DEPENDENCE OF PLANAR ANTENNA RESISTANCE ON PLASMA PARAMETERS

The standing waves excitation enhances the RF energy absorption and leads to a resonant increase of the resistance, introduced by plasma in the antenna circuit. For traditional antennas of $m = 1$ and $m = 0$ modes this was investigated, in particular, in [8, 9]. To clarify the feature of planar antenna characteristics it is necessary to explore the dependence of its resistance on plasma density and magnetic field strength. It is known, that in the helicon discharge plasma density at given external conditions determines self-consistently and takes discrete values. For this reason the exploration of planar antenna characteristics was carried out in independently formed plasma which concentration can be changed arbitrarily.

2.1. EXPERIMENTAL SETUP AND METHOD OF MEASUREMENTS

In independently produced plasma it was studied the absorption of a weak (< 1 W) signal of frequency 13.56 MHz due to helicon $m = 0$ wave excitation by the planar antenna. This signal does not create an additional ionization and does not affect the spatial density distribution. The experimental setup is shown in Fig. 6.

Plasma was produced in the volume (1) by the electron-cyclotron resonance (ECR) discharge at frequency 2.45 GHz in the magnetic field 87.5 mT. Then, through the limiting grid (9) made of perforated copper sheet, plasma came into the experimental volume (2). Geometrical dimensions of this volume were identical to the previous device (see Fig. 1), except that the metal section and quartz chamber exchanged their positions. Subsequent experiments were conducted at argon pressure of 90 mPa, preferable for the ECR source operation. At higher pressures (0.65 Pa) the discharge concentrates in the plasma source volume and badly penetrates into the experimental chamber.

Between the plasma source and the chamber a ferromagnetic shield was installed that reduced the spreading of strong magnetic field from ECR zone into the experimental volume. An adjustable homogeneous magnetic field was formed by coils (3). The averaged over the cross section plasma density was measured with the 8-mm microwave interferometer (8).

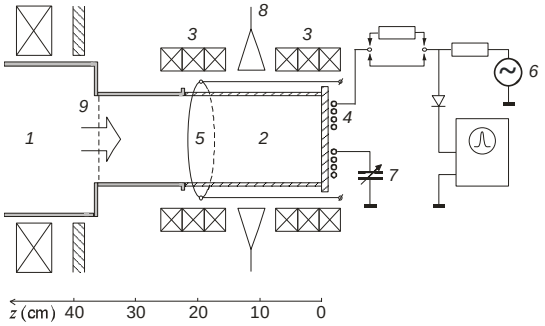

Fig. 6. Experimental device for measurement of antenna resistance at the helicon waves excitation in independently produced ECR plasma: 1 – ECR plasma source (F = 2.45 GHz, B_0 = 87.5 mT, W = 800 W); 2 – experimental volume; 3 – magnetic field coil; 4 – planar m = 0 antenna; 5 – frame m = 1 antenna; 6 – signal generator (f = 13.56 MHz, W ≤ 1 W); 7 – serial capacitor; 8 – microwave interferometer (f = 35 GHz); 9 – limiting grid-reflector. p_{Ar} = 0.09 Pa

At the end of the quartz chamber the planar antenna (4) of previously described design was placed. To compare characteristics of different antennas the chamber was also equipped with the frame antenna (5) of $m = 1$ mode, which length 18 cm occupied a half of the chamber length, and a one-turn loop antenna $m = 0$, which embraced the chamber at $Z = 7$ cm (not shown in figure). The method used for measurement of an inductive antenna resistance due to plasma load was described in [9]. The antenna inductance together with the variable capacitor (7) formed a serial resonant circuit, which impedance in the resonance is equal to the real antenna resistance. This circuit is a part of the voltage divider, which is powered with a fixed voltage from the signal generator (6) at a frequency 13.56 MHz. The voltage drop across the circuit at resonance is proportional to the sum of the own antenna resistance and the resistance, introduced in the antenna circuit by a plasma load.

After detecting this voltage drop was registered by an oscilloscope. The oscilloscope deviations were calibrated in Ohms by including to the antenna circuit of permanent resistors of known values without plasma. The magnetron of ECR plasma source was working in pulsed-periodic mode with repetition frequency of

50 Hz. During each pulse the plasma density increased from zero to the maximum value and then decreased to zero. Thus, for a given magnetic field B_0 on the oscilloscope screen we directly observed the dependence of the antenna resistance on plasma density, which was measured by the microwave interferometer (8) for any moment of time.

2.2. EXPERIMENTAL RESULTS

Fig. 7 shows the dependence of the 4-turn planar antenna resistance on the diametrically averaged plasma density at different magnetic fields – 1.5, 3.0, 4.5, 7.5 and 9.0 mT. Only coordinates of the specific points – maximums and minimums–were measured, which then were connected by a curve, similar to observed on the scope screen. Since the presence of plasma to some extent influenced also a reactive component of impedance (inductance), the value of the variable capacitor (7) was adjusted to the resonance at every

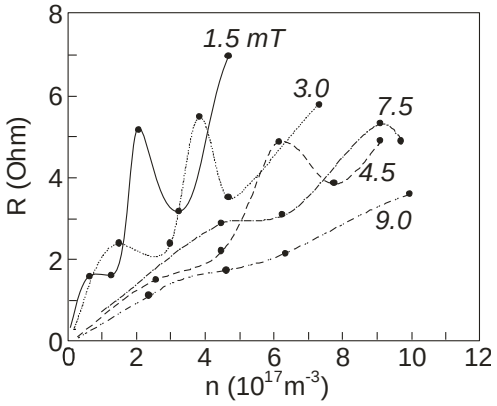

Fig. 7. Dependence of the planar antenna resistance on ECR plasma density at different magnetic fields

point that was determined by the minimum amplitude across the circuit. Note that the maximal plasma density penetrated into the experimental volume strongly depends on the magnetic field in the chamber. With increasing field B_0 the plasma density also increases, but more slowly than the field strength increases. Therefore, the largest ratio of density to magnetic field n/B_0 is achieved at lower magnetic fields.

The dependence of the planar antenna resistance on density, shown see in Fig. 7, is strongly non-monotonous. The reason is that in the resonant conditions the excitation of standing helicon waves arises, the RF energy absorption and, consequently, the real antenna impedance increases. With increasing magnetic field the resonance shifts to higher densities according to the helicon wave dispersion. Since the wavelength λ reduces with increasing density, the peaks see in Fig. 7 apparently correspond to resonances of the first and second axial cavity modes. At the same time, in the helicon discharge (see Fig. 2 and Fig. 3) we have observed the higher standing wave modes (from 3rd to 6th). This difference is due to lower values of the parameter n/B_0, which can be achieved in our device with ECR discharge comparing to the real helicon discharge.

Analysis of see Fig. 7 shows that the resonances, obtained at different values of n and B_0 are observed at about the same values of n/B_0, This makes it possible to compare the characteristics of various antennas as depending on this parameter. In Fig. 8 the 4-turn planar antenna resistance is shown by the solid curve 1. The curve 2 shows the resistance of a one-loop $m = 0$ antenna, located in the plane $Z = 7$ cm. The dashed curve 3 corresponds to the frame $m = 1$ antenna, shown see in Fig. 6. As is seen from Fig. 8 the highest quality, i.e. the ratio of resonant and off-resonance impedances shows the second resonance of the loop $m = 1$ antenna.

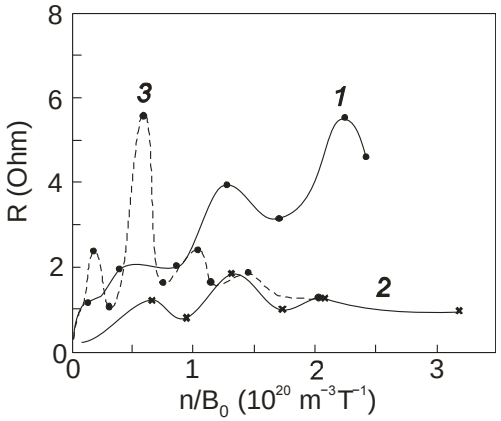

Fig. 8. Resistances of different type antennas as function of the parameter n/B_0: 1 – 4-turn planar m = 0 antenna; 2 – one-turn m = 0 loop antenna; 3 – the frame m = 1 antenna 18 cm long, which occupies a half of the experimental chamber length. p_{Ar} = 0.09 Pa

This is because for this antenna the second cavity mode of axial standing wave coincides with the own antenna resonance, and so this double-resonance manifests particularly clearly. In contrast, the planar and the loop $m = 0$ antennas have not their own resonances and exhibit only cavity modes with lower quality.

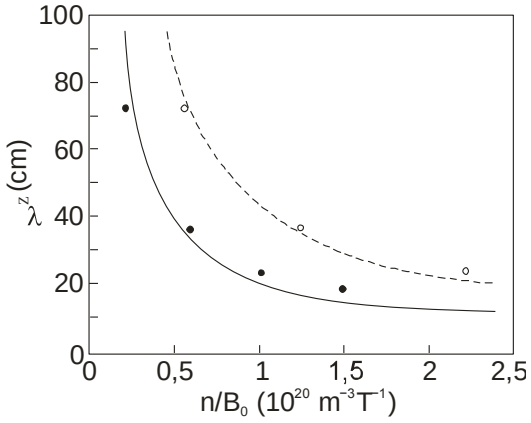

Fig. 9. Positions of the planar antenna resonances (light circles) and the frame antenna resonances (dark circles) relative to theoretical dispersion properties of the first radial $n_r = 1$, m = 1 mode (solid curve) and the second radial $n_r = 2$, m = 0 mode (dashed curve) in a cylindrical plasma column of radius a = 6 cm and of length 36 cm

The most significant difference in these characteristics is that the same 1st, 2nd and 3rd resonances of the $m = 0$ antennas are observed at about two times larger values of the parameter n/B_0, than for the frame $m = 1$ antenna. By the way, this explains why in [9], were the dependence of resistance on density was studied at a fixed magnetic field, resonant properties of the loop $m = 0$ antenna were not revealed. The chosen there magnetic field 11.5 mT at a density of 10^{18} m^{-3} corresponded to the value $n/B_0 \le 10^{20}$ m^{-3}T^{-1}, where the $m = 0$ antenna demonstrates only the vague first resonance, while the antenna $m = 1$ in this region shows three distinct resonances.

This feature of the $m = 0$ mode may be explained by supposing that the planar antenna and loop $m = 0$ antenna both excite the second radial mode. Considering the results of see Fig. 4 this assumption is rather reasonable.

Fig. 9 shows the dispersion properties of helicon waves propagating in a cylindrical column of radially homogeneous plasma 12 cm in diameter (the inner diameter of our discharge chamber was 14 cm).

Dependences of wavelength λ_Z on n/B_0 were calculated using the dispersion equation for helicon waves

$$kk_z = \frac{\omega_0^2}{c^2}\frac{\omega}{\omega_e}, \qquad (1)$$

with the boundary conditions [1]

$$mkJ_m(k_r a) + k_z J'_m(k_r a) = 0, \qquad (2)$$

where $k^2 = k_z^2 + k_r^2$ – is the total wave number, ω_e, ω_0 – are electron cyclotron and plasma frequencies, J_m, J'_m – Bessel function and its derivative. For the first azimuthal mode ($m = 1$, $n_r = 1$) we used a numerical solution of equation (2) given in [1]. The solid curve in see Fig. 9 shows the dispersion of this mode. The dashed line represents dispersion of the second radial mode of azimuthally symmetric wave ($m = 0$, $n_r = 2$). In this case equation (2) reduces to $J_0' = -J_1 = 0$ and the radial wave number was taken equal to $k_r = 7{,}016/a$, where a – is the plasma radius, and 7,016 – the second root of Bessel function J_1. The points on the graph show the experimentally determined resonances. The wavelength of i-th resonance was found from condition $i\lambda_i/2 = L$. Since the experimental chamber length L was 36 cm, the wavelengths of the first four axial resonances were taken $\lambda_1 = 72$ cm, $\lambda_2 = 36$ cm, $\lambda_3 = 2L/3 = 24$ cm and $\lambda_4 = 18$ cm. The values of parameter n/B_0 that corresponded to individual resonances were taken from the graph see Fig. 8. As shown in Fig.9, the resonances of the frame antenna $m = 1$ (black dots) satisfactorily agree with the main radial mode dispersion, while the planar antenna resonances (light circles) lie closer to the second radial mode $n_r = 2$ of azimuthally symmetric wave $m = 0$.

There is another essential difference of the planar antenna from the conventional antennas $m = 1$ and $m = 0$. With increasing parameter n/B_0 the resistance of traditional frame and loop antennas decreases, while the resistance of planar antenna (at least in the investigated range of parameters) increases, as is seen in see Fig. 8. A possible cause of this resistance reduction in the region of shorter waves is the fallowing. When two adjacent half-waves with opposite field directions get into the near antenna field, their actions mutually compensate. On the contrary, RF magnetic field of the planar antenna, as shown see in Fig. 3, concentrates near the dielectric window at the node of standing wave. In the shorter standing wave its maximum is located closer to the nod and, therefore, the overlapping of antenna fields and wave fields becomes better. Consequently, transition to higher axial modes and to shorter wavelengths improves coupling of the planar antenna with plasma and enhances RF energy deposition in the discharge. Possibly, this explains the relatively higher efficiency of planar antennas for dense plasma generation compared to traditional antennas, that is observed in experiment [8].

CONCLUSIONS

It has been shown that the helicon discharge excited with a flat spiral (planar) antenna in an axially limited volume can exist in discrete states, each corresponding to a particular longitudinal mode of standing helicon waves.

Increasing the external magnetic field at a fixed RF power leads to stepped increase of the standing wave length. After reaching a critical magnetic field, when the waves length becomes comparable to the discharge chamber length, the discharge ceases (breaks down). The critical magnetic field value depends on the available RF power and gas pressure.

In independently produced plasma the resistance, introduced by a plasma load in the planar antenna circuit was measured. It was shown that in the explored range of parameters ($n/B_0 \le 2\times10^{20}$ m^{-3}T^{-1}) with increasing the ratio of plasma density to magnetic field, n/B_0, the resistance of planar antenna increases, unlike the conventional antennas in which this resistance decreases.

It was found that at least the first three resonances, associated with excitation of longitudinal standing modes, in the planar and loop $m = 0$ antennas are observed at about twice larger values of the parameter n/B_0, than for the frame $m = 1$ antenna, that may be due to excitation of higher radial modes.

REFERENCES

1. M.A. Liberman and A.J. Lichtenberg. *Principles of Plasma Discharges and Materials Processing*. New York: “Wiley”, 1994.

2. R.W. Boswell. Very efficient plasma generation by whistler waves near the lower hybrid frequency // *Plasma Phys. and Contr. Fusion.* 1984, v. 26, p. 1147-1162.

3. F.F. Chen. Physics of helicon discharges // *Phys. Plasmas.* 1996, v. 3, p. 1783-1793.

4. J.E. Stevens, M.J. Sowa, J.L. Cecchi. Helicon plasma source excited by a flat spiral coil // *J. Vac. Sci. Technol.* A. 1995, v. 13, p. 2476-2482.

5. S. Shinohara, S. Takechi, Y. Kawai. Effects of axial magnetic field and faraday shield on characteristics of RF produced plasma using spiral antenna //*Japan. J. Appl. Phys.* 1996, v. 35, p. 4503-4508.

6. V.M. Slobodyan, V.F. Virko**,** G.S. Kirichenko, K.P. Shamrai. Helicon discharge excited planar antenna along the magnetic field // *PAST*. 2003, № 4, p. 235-240.

7. T. Motomura, K. Tanaka, S. Shinohara, T. Tanikawa and K.P. Shamrai. Characteristics of large diameter, high-density helicon plasma with short axial length using a flat spiral antenna *// J. Plasma Fusion Res.* 2009, v. 8, p. 6-10.

8. Chi Kyeong-Koo, T.E. Sheridan, R.W. Boswell. Resonant cavity modes of a bounded helicon discharge *// Plasma Sources Sci. Technol.* 1999, v. 8, p. 421-431.

9. V.F. Virko, G.S. Kirichenko, K.P. Shamrai. Geometrical resonances of helicon waves in an axially bounded plasma */Plasma Sources Sci. Technol.* 2002, v. 11, p. 10-26.

Article received 15.09.2014

ГЕЛИКОННЫЙ РАЗРЯД, ВОЗБУЖДАЕМЫЙ ПЛАНАРНОЙ АНТЕННОЙ В ОГРАНИЧЕННОМ ОБЪЁМЕ

В.Ф. Вирко, В.М. Слободян, К.П. Шамрай, Ю.В. Вирко

Прямыми пространственными измерениями высокочастотных волновых магнитных полей подтверждено, что скачкообразные изменения плотности плазмы в геликонном разряде, возбуждаемом плоской (планарной) антенной, вызываются изменением продольных мод стоячих геликонных волн в ограниченном объёме. В независимо приготовленной плазме измерено сопротивление планарной антенны при различных значениях концентрации плазмы n и магнитного поля B_0. В исследованном диапазоне параметров ($n/B_0 \leq 2{,}5\times10^{20}$ м$^{-3}\cdot$Тл$^{-1}$) с увеличением отношения n/B_0 сопротивление планарной антенны растёт, в отличие от геликонных антенн других типов. Резонансы поглощения ВЧ-энергии, вызванные раскачкой стоячих волн, у планарной антенны наблюдаются при значениях n/B_0 вдвое больших, чем у рамочной m = 1 антенны.

ГЕЛІКОННИЙ РОЗРЯД, ЗБУДЖУВАНИЙ ПЛАНАРНОЮ АНТЕНОЮ В ОБМЕЖЕНОМУ ОБ'ЄМІ

В.Ф. Вірко, В.М. Слободян, К.П. Шамрай, Ю.В. Вірко

Прямими просторовими вимірюваннями високочастотних хвильових магнітних полів підтверджено, що стрибкоподібні зміни густини плазми в геліконному розряді, збуджуваному плоскою (планарною) антеною, спричиняються зміною поздовжніх мод стоячих геліконних хвиль в обмеженому об'ємі. У незалежно утвореній плазмі виміряно опір планарної антени при різних значеннях концентрації плазми n та мангітного поля B_0. У дослідженому діапазоні параметрів ($n/B_0 \leq 2{,}5\times10^{20}$ м$^{-3}\cdot$Тл$^{-1}$) зі збільшенням відношення n/B_0 опір планарної антени зростає, на відміну від геліконних антен інших типів. Резонанси поглинання ВЧ-енергії, обумовлені розкачкою стоячих хвиль, у планарної антени спостерігаються при значеннях n/B_0 вдвічі більших, ніж у рамкової m = 1 антени.